FUDMA Journal of Sciences (FJS)
ISSN online: 2616-1370
ISSN print: 2645 - 2944
Vol. 10 No. 23, December, 2026, pp 17 – 24
DOI: https://doi.org/10.33003/fjs-2026-1023-6245

Vegetation Change and Farmland Concentration within Grazing Reserves in Adamawa State, Nigeria

***[1]Isa Sarkinzango, [1]Abubakar Akinyele Musa, [1]Takana Abubakar**

Department of Surveying and Geoinformatics, Modibbo Adama University, Yola, Nigeria

*Corresponding authors' email: sarkinzango@gmail.com

ABSTRACT
Vegetation monitoring can inform pastoral land management only when changes in greenness, seasonal vegetation and mapped cultivation are distinguished. This study reanalysed Landsat-derived vegetation summaries for 2002, 2013 and 2024, five Sentinel-2 monthly vegetation summaries for 2024, and land-cover statistics for ten grazing reserves in Adamawa State, Nigeria. Relative change, annualised loss, loss-to-gain ratios, area-weighted farmland prevalence, concentration and deterministic classification-error scenarios were calculated. High-NDVI cover declined from 337,020.66 to 213,629.85 ha, a 36.61% reduction rather than the previously reported 50%. About 93.76% of this net loss occurred during 2002–2013. Within the pairwise change domain, decreases exceeded increases by 19.57 times over 2002–2024. The ten reserves contained 6,446.07 ha of mapped farmland, equivalent to 17.76% of their reported combined area. Dauchi, Guyaku and Ladde Dan-Kiffi accounted for 61.07% of mapped reserve farmland while occupying 44.26% of assessed reserve area. A conditional reserve-level permutation test found limited size–prevalence association (rho = 0.406; p = 0.248), while concentration equalled 5.78 equally contributing reserves. Monthly vegetation presence ranged from 20.19% in May to 96.74% in November. However, mismatches between pixel counts, area conversion and land-cover summaries prevent the seasonal classification from being treated as an independently validated cultivation map. The results support targeted verification of concentrated cultivation and monitoring of high-NDVI loss, while demonstrating why greenness change alone cannot establish deforestation, unlawful encroachment or conflict causation.

Received: 16 Sept. 2026
Accepted: 06 Nov. 2026
Published: 10 Nov. 2026

Keywords: NDVI, Grazing Reserves, Farmland Concentration, Seasonal Vegetation, Adamawa, Remote Sensing

INTRODUCTION

Grazing-reserve management requires evidence of both vegetation change and the distribution of cultivated land. A regional decline in greenness may indicate changing vegetation conditions, while cultivation within a reserve may affect land available for pastoral use. These measures describe different processes and spatial scales. Rangeland resilience depends on management and access to resources, and livestock mobility depends on the seasonal distribution and accessibility of those resources (Reid et al., 2014; Turner & Schlecht, 2019). For Adamawa State, assessing regional vegetation alongside mapped farmland within individual reserves can therefore help identify locations requiring closer investigation.

The Normalized Difference Vegetation Index (NDVI) provides a repeatable measure of the contrast between red and near-infrared reflectance (Tucker, 1979). It measures spectral greenness rather than land tenure, forage quality or livestock carrying capacity. Vegetation removal, moisture variation, observation timing and sensor differences can all affect the index. Soil-background effects are particularly relevant in sparsely vegetated areas (Huete, 1988). Reviews of ecological applications consequently caution against interpreting NDVI as a universal measure of biomass or degradation (Pettorelli et al., 2005; Xue & Su, 2017; Huang et al., 2021; Zeng et al., 2022). This study therefore examines mapped class membership without converting it to biomass.

Temporal observations can improve the distinction between crops and natural vegetation because their seasonal development may differ. Belgiu and Csillik (2018) evaluated temporal matching for cropland classification, while Ibrahim et al. (2021) examined crop mapping in Nigeria using spectral-temporal information and independent field observations. However, the accuracy achieved in those studies cannot be assigned to a binary vegetation-sequence classifier applied to another area. Mapped cultivation must be distinguished from an independently validated area estimate, which requires an appropriate reference sample (Olofsson et al., 2014).

Comparability between observation dates is also necessary for interpreting vegetation change. Research on Landsat continuity and harmonised Landsat–Sentinel observations shows why sensor selection and processing must be considered in cross-date comparisons (Roy et al., 2016; Claverie et al., 2018; Wulder et al., 2019). Sentinel-2 supports frequent optical observation (Drusch et al., 2012), but cloud and shadow screening remain necessary (Zhu & Woodcock, 2012; Zhu et al., 2015). These requirements provide a basis for auditing processing records; they do not establish that the imagery underlying the available summaries has already passed those checks.

The number and timing of observations constrain the conclusions that can be drawn. Methods such as LandTrendr, trend-and-seasonal decomposition and continuous change detection use denser time series than three epoch summaries (Kennedy et al., 2010; Verbesselt et al., 2010; Zhu & Woodcock, 2014). Three dates permit endpoint comparisons but cannot establish a continuous annual trend or the timing

of a breakpoint. Global and Sudano-Sahelian studies further distinguish gross change, fractional cover and net class balance (Song et al., 2018; Souverijns et al., 2020; Winkler et al., 2021). Accordingly, changes in class totals and pairwise directional changes are analysed separately here.

Climatic variability and land management offer possible explanations for changes in greenness, but their contributions require additional evidence. Studies of Sahelian vegetation relate satellite observations to climatic variation and field measurements (Herrmann et al., 2005; Fensholt et al., 2012; Dardel et al., 2014; Mbow et al., 2015). These findings motivate rainfall and field checks in Adamawa without transferring effect sizes from other locations. Cultivation pressure, forage condition and movement restrictions likewise require separate verification before their relationships with farmer–herder interactions can be assessed (Reid et al., 2014; Turner & Schlecht, 2019).

Local evidence makes the spatial distribution of cultivation particularly relevant. Gailyson et al. (2026) documented declining grassland and expanding cultivation in Dauchi Grazing Reserve. Their study provides a reserve-specific comparison, whereas the present analysis considers how mapped farmland is distributed across ten assessed reserves. Absolute cultivated area and the percentage of a reserve under cultivation answer different management questions: a large reserve with moderate prevalence may contain more farmland than a small reserve with high prevalence. Reporting both measures avoids relying on a state-wide percentage or a single ranking. In Adamawa, Adamu (2023) applied remote sensing and GIS to monitor land-cover change in Girei Forest Reserve. In neighbouring Taraba State, Tijwun (2025) used Landsat imagery and NDVI to examine vegetation change; differences in study area, class definitions and methods limit direct numerical comparison with the present assessment.

The analytical gap addressed here is the joint interpretation of regional greenness change, seasonal vegetation presence and the concentration of mapped farmland across the ten reserves. The available summaries do not by themselves show whether the reserves represent all reserves in Adamawa, whether mapped cultivation is authorised, or which environmental process caused a change in greenness. A useful assessment must therefore make its denominators explicit, separate the evidence domains and identify the conclusions that remain conditional on classification and boundary accuracy.

This study aimed to assess vegetation change and the concentration of mapped farmland within grazing reserves in Adamawa State. Its objectives were to recalculate long-term vegetation changes with explicit denominators; compare the five available seasonal vegetation observations without inferring unobserved monthly behaviour; quantify farmland concentration using both absolute area and reserve-level prevalence; and examine the sensitivity of management priorities to stated classification-error scenarios.

The contribution is an auditable secondary analysis of reported geospatial summaries, rather than a new satellite classification or field survey. Independent reference design remains essential to classification accuracy assessment (Congalton, 1991; Foody, 2002; Pontius & Millones, 2011; Stehman & Foody, 2019). For the aggregate data available here, reserves rather than pixels are the statistical units, avoiding unsupported pixel-level replication (Hurlbert, 1984). Descriptive effects and conditional probability are interpreted together, with the limitations of the assessed set made explicit (Wasserstein & Lazar, 2016).

MATERIALS AND METHODS

Study Design and Evidence Domains

The study is a secondary quantitative analysis of the Adamawa geospatial research documented by Sarkinzango (2026). Three evidence domains were analysed separately: Landsat NDVI-class area for 2002, 2013 and 2024; Sentinel-2 binary vegetation summaries for March, May, October, November and December 2024; and class areas within ten mapped grazing-reserve boundaries. The original reserve data were incomplete for parts of the state, so inference is limited to the ten assessed reserves. No new satellite processing or ground survey was undertaken in this reanalysis.

The original workflow used mosaicking and clipping of Landsat scenes, an NDVI classification, and Google Earth Engine processing of Sentinel-2 surface-reflectance imagery. Earth Engine provides a framework for large-area processing (Gorelick et al., 2017). Here the numerical outputs, rather than a newly produced raster archive, form the analytical dataset. Exact scene identifiers, cloud masks, acquisition dates and a common validity mask were not available for independent reconstruction. These omissions limit inference about environmental causes, despite allowing arithmetic recalculation.

The numerical inputs are the reported area summaries attributed to Sarkinzango (2026). Tables 1–3 retain those reported inputs or quantities calculated from them; Table 4 contains aggregate statistical diagnostics. The ±10% and ±3 percentage-point adjustments are explicitly defined sensitivity scenarios, not additional satellite observations or field measurements. Arithmetic agreement with the reported summaries does not independently establish the accuracy or provenance of the underlying maps. The original thesis tables, raster exports, reserve boundaries and processing records remain necessary for that verification.

Vegetation Change and Temporal Comparison

The three Landsat classes were low NDVI below 0.14, medium NDVI from 0.14 through 0.30, and high NDVI above 0.30. Absolute change was calculated as later area minus earlier area; relative change was 100 times this difference divided by the earlier area. Percentage-point changes used the common NDVI-class total of 3,794,847.66 ha. Annualised absolute loss was the net change divided by the number of years, and compound change was $100 \times [(A_2 / A_1)^{1/t} - 1]$. Annualisation describes average change between endpoints and does not establish a continuous annual trajectory.

Here A_1 and A_2 are the earlier and later class areas, respectively, and t is the interval in years.

Pairwise unchanged, decreased and increased areas were analysed on their own reported domain of 3,794,155.36 ha. Gross turnover was decrease plus increase; the loss-to-gain ratio was decrease divided by increase. The difference of 692.30 ha between this domain and the class-area domain was retained explicitly. A full three-by-three class transition matrix cannot be reconstructed from the three directional totals, so statements about the destinations of lost high-NDVI pixels were not made.

Correct sensor-specific bands are essential. Landsat ETM+ uses red Band 3 and near-infrared Band 4, whereas OLI uses red Band 4 and near-infrared Band 5 (U.S. Geological Survey, n.d.). The source describes Bands 4 and 5 generically. This does not establish that the 2002 computation was wrong, but its processing record requires verification before cross-sensor differences are interpreted as physical change.

Seasonal Presence and Reserve Concentration

For the seasonal summaries, vegetation presence was the reported area above an NDVI threshold of 0.2 divided by the sum of vegetation and non-vegetation area for each month. This creates comparable within-month proportions while preserving the source domain. The five observations do not include June–September and therefore do not resolve the full growing-season trajectory. Binary sequences were audited by summing their pixel counts and checking the implied area per pixel against the stated 10 m export scale.

For each reserve, mapped farmland prevalence was farmland area divided by reported total area. The pooled estimate was the sum of farmland areas divided by the sum of reserve totals; the unweighted mean of the ten percentages was calculated separately. Priority rankings used both absolute farmland area and prevalence. The top-three concentration share was their combined farmland divided by the pooled farmland area. Concentration enrichment was this share divided by their share of assessed reserve area.

Two deterministic checks were used. First, farmland areas were multiplied by 0.9 and 1.1 to represent proportional downward and upward classification adjustments; these are scenarios, not confidence intervals. Second, each reserve prevalence was allowed to vary independently by three percentage points to examine separation between groups. No binomial tests were used because map pixels are spatially dependent and no probability sample of reference labels was available. There is consequently no defensible sampling-based significance test or accuracy-adjusted area interval.

Additional Statistical and Sensitivity Methods

Ten reported reserve totals were used as finite assessment units. Absolute farmland concentration was measured by the Gini coefficient, $G = \frac{2\sum_{i=1}^{n} i\,x_i}{n\sum_{i=1}^{n} x_i} - \frac{n+1}{n}$, with nonnegative areas ordered increasingly. The concentration index $H = \sum_{i=1}^{n} s_i{}^2$, where s is each reserve's farmland share, was also expressed as 1/H effective reserves (Jost, 2006). Median and interquartile range described prevalence. These are descriptive statistics of the assessed set, without sampling confidence intervals.

The association between reserve area and farmland prevalence used Spearman's rho (Spearman, 1904). A two-sided conditional permutation test shuffled the ten prevalence ranks 99,999 times with seed 20261011 and calculated $p = \frac{b+1}{B+1}$, where b counts absolute correlations at least as large as the observed value (Phipson & Smyth, 2010). Its null requires exchangeability across the assessed reserves; purposive selection and spatial dependence may violate this requirement. The result is an exploratory diagnostic conditional on that assumption, not a population inference. Leave-one-reserve-out recalculation evaluated influence on pooled prevalence and association. Kendall rank concordance compared absolute-area and prevalence priorities descriptively.

For an additional reproducibility check using the ten reserve areas and farmland areas in Table 3, the two-sided rank-permutation probability was also evaluated by enumerating all 10! = 3,628,800 assignments. There were 898,022 assignments with an absolute rank correlation at least as large as the observed value, giving an exact conditional probability of 0.24747. This check supports the same interpretation as the reported Monte Carlo estimate of 0.24832. It checks the aggregate calculation, not the original image classification or data provenance.

RESULTS AND DISCUSSION

Long-Term Changes Differ from The Original Percentage Interpretation

Table 1: NDVI-Class Areas and Recalculated Endpoint Change

Class	2002 ha	2013 ha	2024 ha	Net change ha	Relative %
Low	67,889.88	213,933.45	131,024.79	+63,134.91	+93.00
Medium	3,389,937.12	3,359,579.79	3,450,193.02	+60,255.90	+1.78
High	337,020.66	221,334.42	213,629.85	-123,390.81	-36.61

Relative change uses the 2002 class area as denominator. Total mapped area is 3,794,847.66 ha at each date.

High-NDVI cover fell by 123,390.81 ha, or 36.61%, between 2002 and 2024. Its share of the class-area domain declined from 8.88% to 5.63%, a reduction of 3.25 percentage points. The distinction matters: a 36.61% reduction in one class is not a 36.61% reduction in vegetation across the state. Medium-NDVI cover remained dominant, increasing from 89.33% to 90.92%, while low-NDVI cover increased from 1.79% to 3.45%.

The first interval accounted for 115,686.24 ha of high-NDVI loss, compared with 7,704.57 ha in the second. Therefore, 93.76% of the endpoint loss occurred during 2002–2013. Relative high-class reductions were 34.33% and 3.48%, respectively. Average annual absolute losses were approximately 10,516.93 and 700.42 ha. The 22-year compound high-class change was about −2.05% annually. These results describe a strongly uneven temporal pattern, not a constant degradation rate.

The previously reported 50% loss arose from dividing a negative class change by the sum of absolute changes across all classes. Because the net changes sum to zero, the combined gains equal the combined losses. When a single class supplies all net loss, its share of absolute class change is mechanically 50%. That statistic describes redistribution accounting and does not measure the percentage of the initial class that disappeared. The recalculated relative changes avoid this interpretive error.

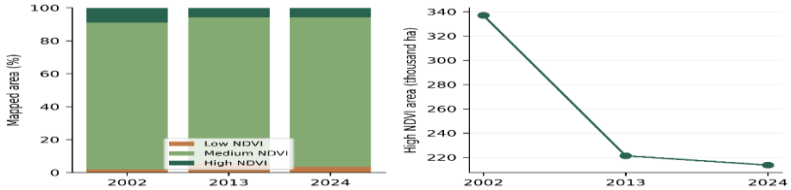


Figure 1: NDVI Composition and High-class Area at the three Observation Dates. Values are Mapped Class Summaries, not Biomass or Forest-area estimates

Directional Change Indicates Extensive Loss but Not an Identified Mechanism

Table 2: Directional Change On the Pairwise Valid Domain

Period	Unchanged %	Decrease %	Increase %	Turnover %	Loss / gain
2002–2013	73.51	23.79	2.70	26.49	8.81
2013–2024	87.19	8.04	4.76	12.81	1.69
2002–2024	72.85	25.83	1.32	27.15	19.57

Over 2002–2024, 25.83% of the pairwise domain decreased and 1.32% increase in vegetation class, producing a loss-to-gain area ratio of 19.57. Gross turnover was 27.15%, while 72.85% retained its class. The first interval had substantially more turnover than the second, consistent with the class-total comparison. However, unchanged class membership does not imply unchanged NDVI within a class. Conversely, a small NDVI fluctuation close to a threshold can move a pixel between categories.

High-class loss is consistent with reduced greenness, but a causal account requires additional variables. The summaries cannot partition agricultural clearing, rainfall anomalies, fire, fuelwood collection or grazing effects. Similarly, loss of a class above 0.30 is not equivalent to deforestation: crops and moist grassland can exceed that threshold, while dry woodland may not. The defensible inference is reduced mapped high greenness within the source processing framework. Identifying the responsible land-cover transitions requires a validated transition matrix and harmonised observations.

Seasonal Observations Reveal a Large Presence Range and A Conversion Audit Problem

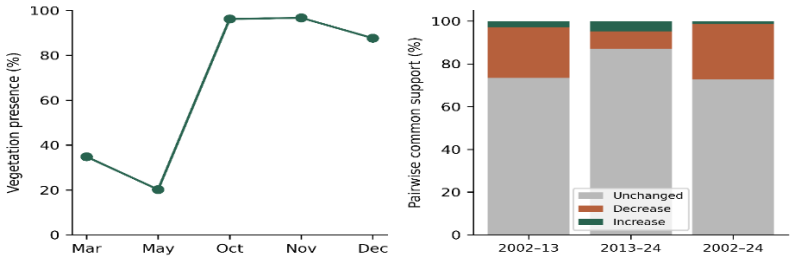


Figure 2: Within-Month Vegetation Presence in 2024 And Directional Change Proportions for The Landsat Comparisons. Each Panel Uses Its Own Documented Domain

Vegetation presence was 34.82% in March, 20.19% in May, 96.21% in October, 96.74% in November and 87.67% in December. The May-to-November difference was 76.55 percentage points. The March-to-May decline contradicts a simple interpretation of steadily improving early-season vegetation. Because observations are separated by unequal intervals, the large May-to-October gain cannot be attributed to an individual month or interpreted as a rate comparable with October-to-November change.

The binary sequence table totals 385,834,969 pixels. At a true 10 m by 10 m projected grid, this corresponds to 3,858,349.69 ha. Reconstructing each month's vegetated pixels yields 1,343,451.82 ha for March and 3,732,541.69 ha for November under that cell size, compared with reported monthly values of 1,084,445.97 and 3,012,987.47 ha. The implied conversion is approximately 0.008072 ha per pixel across months. Reserve count-to-area ratios are about 0.008 ha per pixel. These values could reflect a different projected cell size or area calculation, but the grid metadata are needed to resolve the discrepancy.

Moreover, the sequence-labelled farmland comprises 58.75% of its pixel domain, whereas a separate six-class land-cover summary reports farmland at 10.48%. The domains and class definitions differ, so these percentages cannot be substituted for one another. This discrepancy is not corrected by choosing whichever result better fits an expected narrative. The reserve overlay remains a reported mapped estimate, and the seasonal label rules require independent verification before they are used to infer cultivated area.

Reserve Pressure Is Concentrated and Rankings Depend on the Chosen Metric

Table 3: Mapped Farmland Within the Ten Assessed Reserves

Reserve	Total ha	Farmland ha	Reserve %	Pooled farmland %
Dauchi	5,573.48	1,790.94	32.13	27.78
Guyaku	6,978.88	1,163.45	16.67	18.05
Ladde Dan-Kiffi	3,513.56	982.16	27.95	15.24
Jibro	2,982.19	926.89	31.08	14.38
Shaushau	4,216.09	702.46	16.66	10.90
Daware	4,416.91	402.79	9.12	6.25
Gurin Njamare	7,123.82	371.98	5.22	5.77
Kuva Gaya	1,157.58	101.00	8.73	1.57
Belel Puch	147.69	2.64	1.79	0.04
Yadim	185.04	1.76	0.95	0.03

Mapped farmland totalled 6,446.07 ha within 36,295.24 ha of assessed reserves, giving an area-weighted prevalence of 17.76%. The unweighted mean reserve prevalence was 15.03%. The difference indicates that larger reserves tended to contribute more cultivated area than a simple average of reserve percentages suggests. Neither statistic represents all state reserves because the assessment was restricted by boundary availability.

Dauchi, Guyaku and Ladde Dan-Kiffi contained 3,936.55 ha of mapped farmland. Their 61.07% share of pooled farmland exceeded their 44.26% share of assessed reserve area, giving an enrichment factor of 1.38. These are the leading locations for an area-based verification programme. A prevalence-based programme would instead identify Dauchi, Jibro and Ladde Dan-Kiffi, where cultivation occupied approximately 32.13%, 31.08% and 27.95% of each reserve. Guyaku therefore rises in priority when the management objective is the amount of potentially affected land rather than its percentage.

The finding accords in direction with the independent Dauchi study by Gailyson et al. (2026), but the values differ substantially: their reported 2024 cultivated area was 46.35 km², compared with 17.91 km² here. Their classification and reserve domain also differ. This comparison is evidence for boundary and classification reconciliation, not numerical validation. It strengthens the case for checking Dauchi while preventing a false claim of agreement between incompatible mapped estimates.

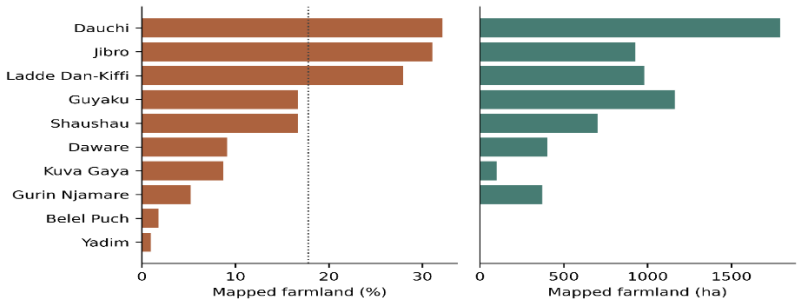


Figure 3: Relative and Absolute Mapped Farmland by Reserve. The Dotted Line Marks Pooled Prevalence, 17.76%; It Is Not a Regulatory Threshold

Sensitivity and Implications for Management

A proportional adjustment of −10% or +10% to mapped farmland changes pooled prevalence to 15.98% or 19.54%, respectively. These scenarios do not estimate classification accuracy; they show that moderate proportional error would preserve the conclusion of appreciable mapped cultivation. A shared proportional adjustment also preserves rankings exactly, so differential error is the more important concern for choosing reserves.

Under independent three-percentage-point shifts, the lowest possible prevalence among Dauchi, Jibro and Ladde Dan-Kiffi is approximately 24.95%, whereas the highest possible prevalence among the remaining seven is approximately 19.67%. Thus, that three-reserve prevalence group remains separated under the stated scenario. Ordering within the group does not remain certain. Dauchi remains first by area under independent ±3 percentage-point shifts, but the ordering of Guyaku, Ladde Dan-Kiffi and Jibro can vary. This supports tiered priorities rather than an overprecise rank order.

The appropriate first intervention is verification of boundary positions, cultivation labels and present land rights. A spectral farmland label does not distinguish authorised cultivation, negotiated use, obsolete boundaries or unlawful occupation. Likewise, shrubland and forest areas cannot simply be added as available grazing: forage accessibility and suitability depend on species, season, water, protected status and management. Policy should consequently use these maps to direct field investigation and dialogue, not to authorise displacement or to assert that reserve creation alone will reduce conflict.

Concentration Association and Influence Diagnostics

Table 4: Reserve-Level Descriptive and Conditional Statistical Diagnostics

Diagnostic	Calculated statistic
Farmland Gini coefficient	0.475
Reserve-area Gini coefficient	0.379
Farmland concentration index H	0.173
Effective farmland-bearing reserves	5.78 of 10
Prevalence median and quartiles	12.89%; 6.10–25.13%
Area–prevalence Spearman rho	0.406
Conditional two-sided permutation p	0.24832
Permutation Monte Carlo standard error	0.00137
Farmland-area versus prevalence Kendall tau	0.822

Farmland is more concentrated than reserve area: its Gini coefficient is 0.475, compared with 0.379 for assessed reserve size. The effective farmland-bearing count is 5.78, meaning that the observed squared-share concentration is equivalent to that of about six equally contributing reserves. This is an allocation summary, not a count of occupied or functioning reserves. The Lorenz comparison uses separate size orderings and therefore describes distributional inequality rather than attributing cultivation to individual reserve size.

Median farmland prevalence is 12.89%, below the pooled 17.76%. Spearman's rho between reserve size and prevalence is 0.406; the conditional permutation probability is 0.248, with Monte Carlo standard error 0.0014. The small assessed set therefore does not provide strong evidence of a monotonic

size–prevalence relationship under the stated exchangeability null. Pearson correlation with $log_{10}(area)$ is 0.578, but the rank result and selection limitations prevent a general claim that larger reserves are intrinsically more exposed.

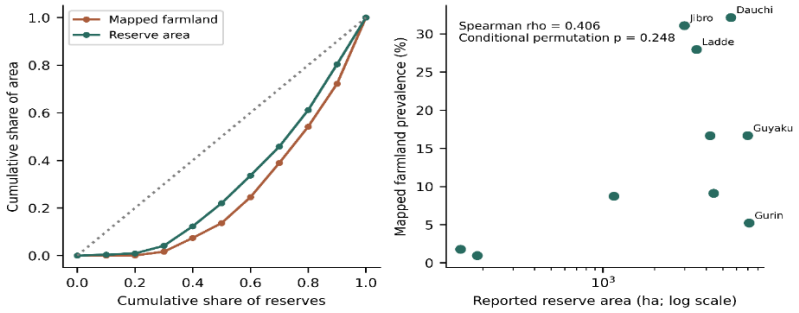


Figure 4: Lorenz Distributions and Reserve Size–Prevalence Association

Leave-one-reserve-out pooled prevalence ranges from 15.15% after removing Dauchi to 20.82% after removing Gurin Njamare. The difference is a leverage diagnostic, not a confidence interval. The association remains positive across omissions, with rho ranging from 0.200 to 0.650, but this does not remove the uncertainty due to non-random reserve selection or classification error. Dauchi's contribution warrants early verification because its removal changes the pooled estimate appreciably, while Gurin's large area and comparatively low prevalence suppress the pooled percentage.

Absolute-area and prevalence rankings have Kendall concordance 0.822. Their substantial overall agreement does not eliminate the specific Guyaku–Jibro priority difference. If the objective is restoring the greatest mapped area, absolute hectares remain appropriate; if the objective is protecting reserve integrity proportionally, prevalence is more relevant. The scenario bars further favour reporting robust priority groups rather than exact ranks. Independent ±3 percentage-point adjustments retain separation of the three highest-prevalence reserves from the rest, while order within that group remains uncertain.

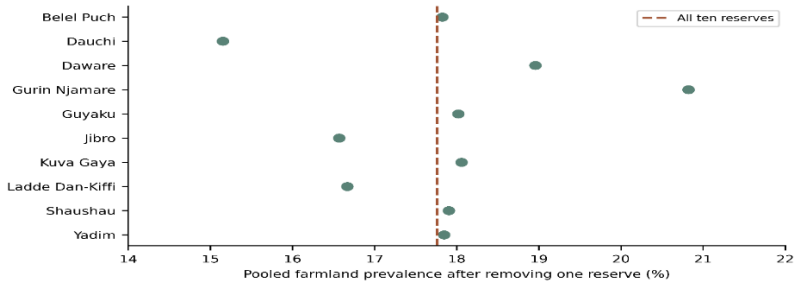


Figure 5: Leave-One-Reserve-Out Pooled Farmland Prevalence

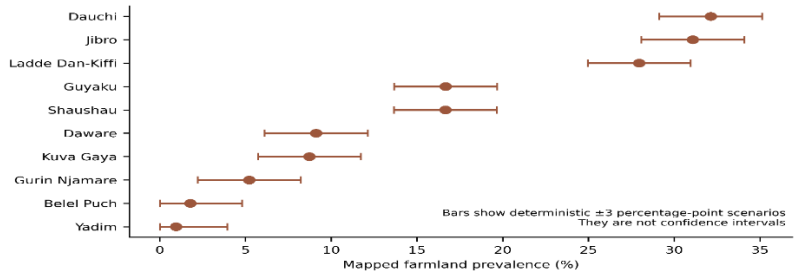


Figure 6: Reserve Prevalence Under Independent ±3 Percentage-Point Classification Scenarios

CONCLUSION

The study found a 36.61% decline in high-NDVI cover between 2002 and 2024, with most of the decline occurring during 2002–2013. The ten assessed grazing reserves contained 6,446.07 ha of mapped farmland, representing 17.76% of their combined area. Cultivation was concentrated within a few reserves, although the analysis did not establish a statistically significant relationship between reserve size and farmland prevalence. Differences between absolute farmland area and percentage coverage show that reserve prioritisation should reflect the specific management objective. These findings support targeted vegetation monitoring, verification of cultivated reserve boundaries and restoration planning in the most affected reserves. Field-based classification validation and consistent spatial processing are necessary to strengthen the mapped estimates and guide management decisions.

REFERENCES

Adamu, S. (2023). Remote sensing and GIS application for forest reserve monitoring and prediction: A case of Girei Forest Reserve, Adamawa State, Nigeria. FUDMA Journal of Sciences, 3(3), 83–94. https://fjs.fudutsinma.edu.ng/index.php/fjs/article/view/1542

Belgiu, M., & Csillik, O. (2018). Sentinel-2 cropland mapping using pixel-based and object-based time-weighted dynamic time warping analysis. *Remote Sensing of Environment, 204*, 509–523. https://doi.org/10.1016/j.rse.2017.10.005

Claverie, M., Ju, J., Masek, J. G., Dungan, J. L., Vermote, E. F., Roger, J. C., Skakun, S. V., & Justice, C. (2018). The Harmonized Landsat and Sentinel-2 surface reflectance data set. *Remote Sensing of Environment, 219*, 145–161. https://doi.org/10.1016/j.rse.2018.09.002

Congalton, R. G. (1991). A review of assessing the accuracy of classifications of remotely sensed data. *Remote Sensing of Environment, 37*(1), 35–46. https://doi.org/10.1016/0034-4257(91)90048-b

Dardel, C., Kergoat, L., Hiernaux, P., Mougin, E., Grippa, M., & Tucker, C. J. (2014). Re-greening Sahel: 30 years of remote sensing data and field observations (Mali, Niger). *Remote Sensing of Environment, 140*, 350–364. https://doi.org/10.1016/j.rse.2013.09.011

Drusch, M., Del Bello, U., Carlier, S., Colin, O., Fernandez, V., Gascon, F., Hoersch, B., Isola, C., Laberinti, P., Martimort, P., Meygret, A., Spoto, F., Sy, O., Marchese, F., & Bargellini, P. (2012). Sentinel-2: ESA's optical high-resolution mission for GMES operational services. *Remote Sensing of Environment, 120*, 25–36. https://doi.org/10.1016/j.rse.2011.11.026

Fensholt, R., Langanke, T., Rasmussen, K., Reenberg, A., Prince, S. D., Tucker, C., Scholes, R. J., Le, Q. B., Bondeau, A., Eastman, R., Epstein, H., Gaughan, A. E., Hellden, U., Mbow, C., Olsson, L., Paruelo, J., Schweitzer, C., Seaquist, J., & Wessels, K. (2012). Greenness in semi-arid areas across the globe 1981–2007 — an Earth Observing Satellite based analysis of trends and drivers. *Remote Sensing of Environment, 121*, 144–158. https://doi.org/10.1016/j.rse.2012.01.017

Foody, G. M. (2002). Status of land cover classification accuracy assessment. *Remote Sensing of Environment, 80*(1), 185–201. https://doi.org/10.1016/s0034-4257(01)00295-4

Gailyson, N. J., Ubogu, A. E., & Abdu, Y. (2026). Land use/land cover dynamics and the decline of grazing resources in Dauchi Grazing Reserve, Adamawa State, Nigeria. *FUDMA Journal of Sciences, 10*(18), 271–276. https://doi.org/10.33003/fjs-2026-1018-6083

Gorelick, N., Hancher, M., Dixon, M., Ilyushchenko, S., Thau, D., & Moore, R. (2017). Google Earth Engine: Planetary-scale geospatial analysis for everyone. *Remote Sensing of Environment, 202*, 18–27. https://doi.org/10.1016/j.rse.2017.06.031

Herrmann, S. M., Anyamba, A., & Tucker, C. J. (2005). Recent trends in vegetation dynamics in the African Sahel and their relationship to climate. *Global Environmental Change, 15*(4), 394–404. https://doi.org/10.1016/j.gloenvcha.2005.08.004

Huang, S., Tang, L., Hupy, J. P., Wang, Y., & Shao, G. (2021). A commentary review on the use of normalized difference vegetation index (NDVI) in the era of popular remote sensing. *Journal of Forestry Research, 32*(1), 1–6. https://doi.org/10.1007/s11676-020-01155-1

Huete, A. R. (1988). A soil-adjusted vegetation index (SAVI). *Remote Sensing of Environment, 25*(3), 295–309. https://doi.org/10.1016/0034-4257(88)90106-x

Hurlbert, S. H. (1984). Pseudoreplication and the design of ecological field experiments. *Ecological Monographs, 54*(2), 187–211. https://doi.org/10.2307/1942661

Ibrahim, E. S., Rufin, P., Nill, L., Kamali, B., Nendel, C., & Hostert, P. (2021). Mapping crop types and cropping systems in Nigeria with Sentinel-2 imagery. *Remote Sensing, 13*(17), Article 3523. https://doi.org/10.3390/rs13173523

Jost, L. (2006). Entropy and diversity. *Oikos, 113*(2), 363–375. https://doi.org/10.1111/j.2006.0030-1299.14714.x

Kennedy, R. E., Yang, Z., & Cohen, W. B. (2010). Detecting trends in forest disturbance and recovery using yearly Landsat time series: 1. LandTrendr — Temporal segmentation algorithms. *Remote Sensing of Environment, 114*(12), 2897–2910. https://doi.org/10.1016/j.rse.2010.07.008

Mbow, C., Brandt, M., Ouedraogo, I., De Leeuw, J., & Marshall, M. (2015). What four decades of earth observation tell us about land degradation in the Sahel?. *Remote Sensing, 7*(4), 4048–4067. https://doi.org/10.3390/rs70404048

Olofsson, P., Foody, G. M., Herold, M., Stehman, S. V., Woodcock, C. E., & Wulder, M. A. (2014). Good practices for estimating area and assessing accuracy of land change. *Remote Sensing of Environment, 148*, 42–57. https://doi.org/10.1016/j.rse.2014.02.015

Pettorelli, N., Vik, J. O., Mysterud, A., Gaillard, J. M., Tucker, C. J., & Stenseth, N. C. (2005). Using the satellite-derived NDVI to assess ecological responses to environmental change. *Trends in Ecology & Evolution, 20*(9), 503–510. https://doi.org/10.1016/j.tree.2005.05.011

Phipson, B., & Smyth, G. K. (2010). Permutation P-values should never be zero: Calculating exact P-values when permutations are randomly drawn. *Statistical Applications in Genetics and Molecular Biology, 9*(1), Article 39. https://doi.org/10.2202/1544-6115.1585

Pontius, R. G., & Millones, M. (2011). Death to Kappa: Birth of quantity disagreement and allocation disagreement for accuracy assessment. *International Journal of Remote Sensing, 32*(15), 4407–4429. https://doi.org/10.1080/01431161.2011.552923

Reid, R. S., Fernández-Giménez, M. E., & Galvin, K. A. (2014). Dynamics and resilience of rangelands and pastoral peoples around the globe. *Annual Review of Environment and Resources, 39*(1), 217–242. https://doi.org/10.1146/annurev-environ-020713-163329

Roy, D. P., Kovalskyy, V., Zhang, H. K., Vermote, E. F., Yan, L., Kumar, S. S., & Egorov, A. (2016). Characterization of Landsat-7 to Landsat-8 reflective wavelength and normalized difference vegetation index continuity. *Remote Sensing of Environment, 185*, 57–70. https://doi.org/10.1016/j.rse.2015.12.024

Sarkinzango, I. (2026). *Developing a sustainable geospatial model for co-habitation between farmers and herders in Adamawa State* [Unpublished doctoral thesis manuscript]. Modibbo Adama University.

Song, X. P., Hansen, M. C., Stehman, S. V., Potapov, P. V., Tyukavina, A., Vermote, E. F., & Townshend, J. R. (2018). Global land change from 1982 to 2016. *Nature, 560*(7720), 639–643. https://doi.org/10.1038/s41586-018-0411-9

Souverijns, N., Buchhorn, M., Horion, S., Fensholt, R., Verbeeck, H., Verbesselt, J., Herold, M., Tsendbazar, N. E., Bernardino, P. N., Somers, B., & Van De Kerchove, R. (2020). Thirty years of land cover and fraction cover changes over the Sudano-Sahel using Landsat time series. *Remote Sensing, 12*(22), Article 3817. https://doi.org/10.3390/rs12223817

Spearman, C. (1904). The proof and measurement of association between two things. *The American Journal of Psychology, 15*(1), 72–101. https://doi.org/10.2307/1412159

Stehman, S. V., & Foody, G. M. (2019). Key issues in rigorous accuracy assessment of land cover products. *Remote Sensing of Environment, 231*, Article 111199. https://doi.org/10.1016/j.rse.2019.05.018

Tijwun, E. S. (2025). Decadal spatio-temporal dynamics of vegetation change across ecological gradients in Southern Taraba, Nigeria (2014–2024). International Journal of Innovative Science and Research Technology, 10(9), 2486–2490. https://doi.org/10.38124/ijisrt/25sep1401

Tucker, C. J. (1979). Red and photographic infrared linear combinations for monitoring vegetation. *Remote Sensing of Environment, 8*(2), 127–150. https://doi.org/10.1016/0034-4257(79)90013-0

Turner, M. D., & Schlecht, E. (2019). Livestock mobility in sub-Saharan Africa: A critical review. *Pastoralism, 9*(1), Article 13. https://doi.org/10.1186/s13570-019-0150-z

U.S. Geological Survey. (n.d.). *What are the band designations for the Landsat satellites?* https://www.usgs.gov/faqs/what-are-band-designations-landsat-satellites

Verbesselt, J., Hyndman, R., Newnham, G., & Culvenor, D. (2010). Detecting trend and seasonal changes in satellite image time series. *Remote Sensing of Environment, 114*(1), 106–115. https://doi.org/10.1016/j.rse.2009.08.014

Wasserstein, R. L., & Lazar, N. A. (2016). The ASA statement on p-values: Context, process, and purpose. *The American Statistician, 70*(2), 129–133. https://doi.org/10.1080/00031305.2016.1154108

Winkler, K., Fuchs, R., Rounsevell, M., & Herold, M. (2021). Global land use changes are four times greater than previously estimated. *Nature Communications, 12*(1), Article 2501. https://doi.org/10.1038/s41467-021-22702-2

Wulder, M. A., Loveland, T. R., Roy, D. P., Crawford, C. J., Masek, J. G., Woodcock, C. E., Allen, R. G., Anderson, M. C., Belward, A. S., Cohen, W. B., Dwyer, J., Erb, A., Gao, F., Griffiths, P., Helder, D., Hermosilla, T., Hipple, J. D., Hostert, P., Hughes, M. J., … Zhu, Z. (2019). Current status of Landsat program, science, and applications. *Remote Sensing of Environment, 225*, 127–147. https://doi.org/10.1016/j.rse.2019.02.015

Xue, J., & Su, B. (2017). Significant remote sensing vegetation indices: A review of developments and applications. *Journal of Sensors, 2017*, Article 1353691. https://doi.org/10.1155/2017/1353691

Zeng, Y., Hao, D., Huete, A., Dechant, B., Berry, J., Chen, J. M., Joiner, J., Frankenberg, C., Bond-Lamberty, B., Ryu, Y., Xiao, J., Asrar, G. R., & Chen, M. (2022). Optical vegetation indices for monitoring terrestrial ecosystems globally. *Nature Reviews Earth & Environment, 3*(7), 477–493. https://doi.org/10.1038/s43017-022-00298-5

Zhu, Z., & Woodcock, C. E. (2012). Object-based cloud and cloud shadow detection in Landsat imagery. *Remote Sensing of Environment, 118*, 83–94. https://doi.org/10.1016/j.rse.2011.10.028

Zhu, Z., & Woodcock, C. E. (2014). Continuous change detection and classification of land cover using all available Landsat data. *Remote Sensing of Environment, 144*, 152–171. https://doi.org/10.1016/j.rse.2014.01.011

Zhu, Z., Wang, S., & Woodcock, C. E. (2015). Improvement and expansion of the Fmask algorithm: Cloud, cloud shadow, and snow detection for Landsats 4–7, 8, and Sentinel 2 images. *Remote Sensing of Environment, 159*, 269–277. https://doi.org/10.1016/j.rse.2014.12.014

©2026 This is an Open Access article distributed under the terms of the Creative Commons Attribution 4.0 International license viewed via https://creativecommons.org/licenses/by/4.0/ which permits unrestricted use, distribution, and reproduction in any medium, provided the original work is cited appropriately.